Original Article

Integrated analysis and knockdown of *RAB23* indicate the role of *RAB23* in gastric adenocarcinoma

Hui Chen, Dun Pan, Zhihuang Yang, Liangqing Li

Department of Gastrointestinal Surgery, The First Affiliated Hospital of Fujian Medical University, Fuzhou 350000, China

Contributions: (I) Conception and design: H Chen, L Li; (II) Administrative support: L Li; (III) Provision of study materials or patients: D Pan; (IV) Collection and assembly of data: Z Yang; (V) Data analysis and interpretation: H Chen, D Pan; (VI) Manuscript writing: All authors; (VII) Final approval of manuscript: All authors.

Correspondence to: Liangqing Li. Professor, Department of Gastrointestinal surgery, The First Affiliated Hospital of Fujian Medical University, No. 20, Chazhong Road, Taijiang District, Fuzhou 350000, China. Email: liangqingli_doctor@126.com.

Background: The present study aimed to identify key differentially expressed genes (DEGs) and miRNAs (DEmiRNAs) in gastric adenocarcinoma.

Methods: We performed integrated analysis to determine DEGs and DEmiRNAs of gastric adenocarcinoma based on the GEO database. A DEmiRNA-target interaction network was established. GO and KEGG pathway enrichment analyses were utilized. Then, MKN45 cells were transfected with shRNA-*RAB23* to knock down the expression of *RAB23*. CCK-8, transwell and flow cytometry assays were utilized to measure the capacities for cell proliferation, migration and apoptosis, and the apoptosis-related gene and protein levels were measured by using polymerase chain reaction (PCR) and Western blot, respectively. Colocalization analysis of Snc1 with the vesicular protein VAMP3 and the endoplasmic reticulum protein Calnexin was performed to assess the influence of *RAB23* on vesicle transport. Finally, we performed metabolomic analysis by using gas chromatography mass spectrometry (GC-MS).

Results: We performed MMIA of gastric adenocarcinoma based on two miRNA datasets and two mRNA datasets. A total of 4,586 DEmRNAs and 30 DEmiRNAs were obtained. The DEmRNAs of gastric adenocarcinoma were significantly enriched in PI3K/Akt signaling. We identified three interactions, hsa-miR-23a-3p-*PTPN4*, hsa-miR-20b-5p (hsa-miR-130a-3p)-*TNFRSF10B*, and hsa-miR-130a-3p (hsa-miR-363-3p)-*RAB23*, that may be related to the pathogenesis of gastric adenocarcinoma. The growth of MKN45 cells was inhibited by *RAB23* knockdown via shRNA-*RAB23* transfection. Metabolic analysis of three groups revealed a number of significantly altered metabolites, including glycerol, niacinamide, and nonadecanoic acid methylester.

Conclusions: *RAB23* might be a target gene of hsa-miR-130a-3p and hsa-miR-363-3p. In gastric adenocarcinoma cells, knockdown of *RAB23* inhibited cell proliferation, migration, and invasion and increased apoptosis by downregulating the PI3K/Akt pathway.

Keywords: Integrated analysis; *RAB23*; gastric adenocarcinoma; PI3K/Akt pathway

Submitted Aug 13, 2019. Accepted for publication Nov 05, 2019.
doi: 10.21037/atm.2019.11.130
View this article at: http://dx.doi.org/10.21037/atm.2019.11.130

Introduction

Gastric cancer, a common and pernicious disease, is the third most common cause of cancer death worldwide. Morbidity and mortality differ geographically, with East Asia having the highest mortality and morbidity (1,2). The 5-year survival rate is more than 90% if the tumor is diagnosed at a very early stage and resected. Nevertheless, early stages of gas chromatography (GC) are usually asymptomatic, and if patients are diagnosed at advanced stage, the 5-year survival rate is reduced to

20% (3). Therefore, the development of early noninvasive biomarkers is essential for the early diagnosis of GC, which may improve the prognosis of GC.

Gastroscopy is widely used for early screening, but it is invasive, uncomfortable and expensive. Some valid ways to enhance prognosis are to identify early cancerous changes and metastases, to study the molecular mechanism of cancer occurrence, and to find biomarkers for the early diagnosis of GC. *RAB23* is associated with the occurrence and metastasis of tumors (4). Recently, numerous studies have indicated that RAB23 is upregulated in renal cell carcinoma (5), hepatocellular carcinoma (6), osteosarcoma (7), esophageal squamous cell carcinoma (8) and bladder cancer (9), which are regulated by miR-384, miR-16, miR-802, miR-665 and miR-92b. According to our integrated microarray analysis, *RAB23* is upregulated in the tissues of patients with gastric adenocarcinoma and involved in the PI3K-Akt signaling pathway and intracellular vesicle processes. Furthermore, *RAB23* was a predicted target of hsa-miR-130a-3p and hsa-miR-363-3p and was dysregulated in the tissues of patients with gastric adenocarcinoma. To further research the roles of *RAB23* in gastric adenocarcinoma, MKN45 cells were transfected with shRNA-*RAB23* to inhibit the expression of *RAB23*.

Thus, we aimed to determine the expression of *RAB23* in GC, analyze the association between *RAB23* expression and tumor progression, and further explore the possible underlying mechanism. We found that *RAB23* was elevated in GC, was related to the diagnosis of GC, and was regulated by hsa-miR-130a-3p and hsa-miR-363-3p and that *RAB23* knockdown by shRNA interference reduced proliferation and migration and enhanced apoptosis by suppressing the activation of PI3K/Akt signaling in gastric cancer.

Methods

Identification of differentially expressed mRNAs (DEmRNAs) and miRNAs (DEmiRNAs)

Based on the GEO database, we downloaded mRNA data from 104 samples (75 tumor tissues and 29 normal tissues) and miRNA data from 79 samples, including 66 tumor tissues and 13 normal tissues. MetaMA is an R package that performs meta-analysis methods for microarrays. The method used to merge p values was the inverse normal method. Multiple comparisons correction was performed to obtain the values of the false discovery rate (FDR) with the Benjamini & Hochberg method (10).

Protein-protein interaction (PPI) network

Next, we established the PPI network by using Biological General Repository for Interaction Datasets (BioGRID) (11) and Cytoscape (12) on the top 50 DEmRNAs between tumor tissues and normal tissues. Proteins with a degree of ≥30 were defined as hub proteins of the PPI network.

Detection of DEmiRNAs

To further investigate the correlation between DEmiRNAs and DEmRNAs, we obtained DEmiRNA-DEmRNA interaction pairs (including downregulated DEmiRNA-upregulated DEmRNA pairs and upregulated DEmiRNA-downregulated DEmRNA pairs) in tumor tissues *vs.* normal tissues. Detection of the target gene was performed as previously described (13).

Functional annotation of target genes

To explore the biological function of the target genes, we used WebGestalt to analyze all the DEmRNAs and target genes identified via the GO functional classification and the KEGG biochemical pathway analyses (http://www.webgestalt.org/option.php) (14).

Survival analysis for RAB23

The prognostic value of *RAB23* was analyzed using OncoLnc (http://www.oncolnc.org/). Patients were divided into high-level and low-level groups based on the median value of *RAB23*. The overall survival (OS) rates of the patients in the high-level and low-level *RAB23* groups were evaluated using Kaplan-Meier analysis (gepia.cancer-pku.cn/detail.php?gene=&clicktag=survival).

Cell culture

To validate the effect of selected DEmiRNAs and DEmRNAs on gastric cancer cells *in vitro*, we obtained the human gastric cancer cell line MKN45 from the Key Laboratory of Digestive Tract Malignancy, Ministry of Education of Fujian Medical University (Shanghai, China). Cells were transfected with shRNA-*RAB23* (*RAB23* knockdown, *RAB23*-KD) or shRNA negative control (NC). Cells with no treatment were used to determine background

effects (the blank group).

Plasmid construction and transfection

Total RNA was isolated from MKN45 cells and reverse transcribed into complementary DNA (cDNA). The primer sequences of *RAB23* were 5′-TGACTGCGCACTTGGAATAGT-3′ (forward) and 5′-CATAACCACGGGGCCCTAAG-3′ (reverse). The sequences of shRNA-7350, shRNA-7351, shRNA-7352 and shRNA-7353 were obtained from Oligobio. Cells were transfected with shRNA-7350, shRNA-7351, shRNA-7352 and shRNA-7353 or shRNA NC.

Cell proliferation, migration and apoptosis assays

Cell viability was detected using the Cell Counting Kit-8 (CCK-8) (Sigma-Aldrich, USA). We added 10 μL of the CCK8 reagent (Solarbio Science & Technology, Beijing, China) to every well, and then the cells were incubated for 90 min at 37 ℃. We measured the OD value at 450 nm every 24 h (15).

We used transwell chambers to evaluate cell migration and invasion. Cells were digested with trypsin and resuspended in culture medium without serum, and approximately 1×10^4 cells were added to the upper chamber. Subsequently, the cells were incubated for 24 h, and the invasive cells were fixed using 4% paraformaldehyde and then stained with 0.1% crystal violet for 5 min. Finally, we imaged and counted the invasive cells.

Flow cytometry was utilized to evaluate cell apoptosis via the Annexin V-FITC-PI Apoptosis Detection Kit. Cells were analyzed via a FACSCalibur and a BD FACSDiva.

Quantitative reverse transcription PCR (RT-PCR) and Western blot

Using the SYBR Master Mixture, we detected the expression of mRNAs. Western blot assays were performed to detect the relative expression of RAB23, Bcl-2, Rac1 and PI3K. RIPA Lysis Buffer was utilized to lyse cells to extract proteins. This assay was performed as previously described (16).

Metabolomic analysis of gastric cancer cells using gas chromatography mass spectrometry (GC-MS)

To identify the influence of *RAB23* on the metabolism of gastric cancer cells, we performed GC-MS analysis by using a GCMS-QP2010 Ultra with a DB-5MS capillary column. The temperature programming was as follows: the initial temperature of the column oven was 90 ℃; the temperature was kept here for 0.2 min and then was increased by 10 ℃/min to 180 ℃, 5 ℃/min to 240 ℃, and 20 ℃/min to 280 ℃; the temperature was then held at 280 ℃ for 11 min. The raw data from the GC/MS experiments were imported into the Shimadzu GC solution software for analysis, including peak extraction, denoising, and deconvolution, and metabolites were characterized using the Fiehn Lab database.

Immunofluorescence

To assess the influence of *RAB23* on vesicle transport, we performed colocalization analysis of Snc1, the vesicular protein VAMP3 and the endoplasmic reticulum protein Calnexin. Cells were fixed in 4% paraformaldehyde for 15 min and then incubated at 4 ℃ in PBS with 0.5% Triton X-100 for 3 min. Subsequently, 3% bovine serum albumin was used to block cells three times (5 min per time) at room temperature in PBS. We used immunofluorescence to detect protein expression at 4 ℃ overnight. Next, cells were incubated with secondary antibodies for 30 min at room temperature. Nuclei were counterstained with DAPI (Beyotime; Shanghai, China), and images were captured using an upright fluorescence microscope (DM3000; Leica, Solms, Germany) at room temperature (17).

Results

Identification of DEmRNAs and DEmiRNAs between gastric carcinoma tissues and adjacent normal tissues

Two datasets (GSE79973 and GSE13861) of mRNAs and two datasets (GSE94882 and GSE26595) of miRNAs were used in our study. Compared with adjacent normal tissues, 4,586 DEmRNAs were identified in tumor tissues, including 2,606 upregulated DEmRNAs and 1,980 downregulated DEmRNAs. The top 100 upregulated and downregulated DEmRNAs are displayed in *Figure S1A*. Furthermore, a total of 30 DEmiRNAs (15 upregulated and 15 downregulated) were obtained. A hierarchical clustering map of DEmiRNAs is shown in *Figure S1B*. The details of the top 20 DEmRNAs and DEmiRNAs between gastric carcinoma tissues and adjacent normal tissues are shown in *Tables S1*,*S2*.

PPI network

The PPI network consisted of 586 nodes and 650 edges (*Figure S2*). Five hub proteins, including ENO1 (degree =69), HDGF (degree =66), CDK4 (degree =50), KPNA2 (degree =45) and ATP4A (degree =32), were identified according to the PPI network.

DEmiRNA-DEmRNA interaction network

A total of 5,091 DEmiRNA-DEmRNA pairs were obtained (*Figure 1*). Among these, 705 downregulated DEmiRNA-upregulated DEmRNA pairs and 592 upregulated DEmiRNA-downregulated DEmRNA pairs were predicted by ≥4 algorithms, and 667 validated downregulated DEmiRNA-upregulated DEmRNA pairs (*Figure 1A*) and 302 upregulated DEmiRNA-downregulated DEmRNA pairs (*Figure 1B*) were derived from miRWalk. Among these, hsa-miR-130a-3p (18) and hsa-miR-363-3p (19) were predicted to regulate the expression of *RAB23* and were found to be related to gastric cancer after searching the literature. Therefore, *RAB23* was selected as the focus of subsequent experiments.

Functional annotation of DEmiRNA targets

In *Figure 2A,B,C*, based on the GO enrichment analysis, cell proliferation (FDR =0), regulation of cell proliferation (FDR =2.85E-12), vesicle-mediated transport (FDR =0.003872877), endoplasmic reticulum (FDR =0), catalytic complex (FDR =5.72E-14), cytoplasmic vesicle (FDR =6.95E-12) and intracellular vesicle (FDR =6.95E-12) were the most significantly enriched GO terms in gastric cancer. The PI3K-Akt signaling pathway (FDR =0.002893618) and ECM-receptor interaction (FDR =0.002893618) were two significantly enriched pathways in gastric cancer (*Figure 2D*). *TNFRSF10B* (20) and *HIPK2* (20,21) were enriched in the cell proliferation and regulation of cell proliferation terms. *RAB23* (22) was enriched in the cytoplasmic vesicle and intracellular vesicle terms. The Kaplan-Meier survival curves of 378 GC cases showed that *RAB23* was not significantly (P=0.0921) related to the prognosis of GC (*Figure S3*).

RAB23 knockdown inhibits the growth capacity and cell migration of gastric cancer in vitro

We transfected the gastric cancer cell line MKN45 with shRNA-7350, shRNA-7351, shRNA-7352 and shRNA-7353 or shRNA NC to inhibit the expression of *RAB23*. The expression level of *RAB23* was significantly blocked by shRNA-7351 and shRNA-7353 in MKN45 cells (P<0.01, *Figure 3A*), and shRNA-7353 (*RAB23* knockdown, *RAB23*-KD) was used for subsequent experiments.

To examine the proliferative effect of *RAB23* on gastric cancer cells, we utilized the gastric cancer cell line MKN45 for transfection with *RAB23* shRNA-7353 to inhibit the expression of *RAB23*. Cell proliferation was determined by CCK8 assay. As presented in *Figure 3B*, the cell viability was decreased in *RAB23*-deficient MKN45 cells.

A transwell assay was performed to determine whether *RAB23* affected tumor metastasis. As shown in *Figure 3C*, cell migration was slightly decreased in MKN45 cells. We observed that the *RAB23*-knockdown group did not have a changed apoptosis rate compared with the NC group or blank group (P>0.05, *Figure 3D*).

RAB23 knockdown inhibits the activation of the PI3K/Akt pathway in gastric cancer

To investigate the mechanism by which *RAB23* affects gastric cancer progression, we investigated the changes in the PI3K/Akt pathway after *RAB23* knockdown in MKN45 cells. As the qPCR and Western blot results suggest, *RAB23* knockdown significantly reduced the expression level of Bcl-2 and the tumor angiogenesis-promoting protein Rac1. There was no significant change in the level of PI3K protein or PI3K phosphorylation, *RAB23* knockdown also significantly reduced the expression of CD44v6, MMP9 and VEGF (*Figure 4*). Additionally, immunofluorescence staining revealed that *RAB23* influenced vesicle transport (*Figure 5*).

GC/MS metabolic profiling

Typical GC/MS TIC chromatograms of MKN45 cells with three different treatments and the matched normal control are shown in *Figure 6A*. As shown in *Figure 6B*, a total of 56 endogenous metabolites, including glycerol, niacinamide, and nonadecanoic acid methylester, were detected sequentially.

Discussion

Despite the development of diagnostic techniques and treatment methods for gastric adenocarcinoma, most

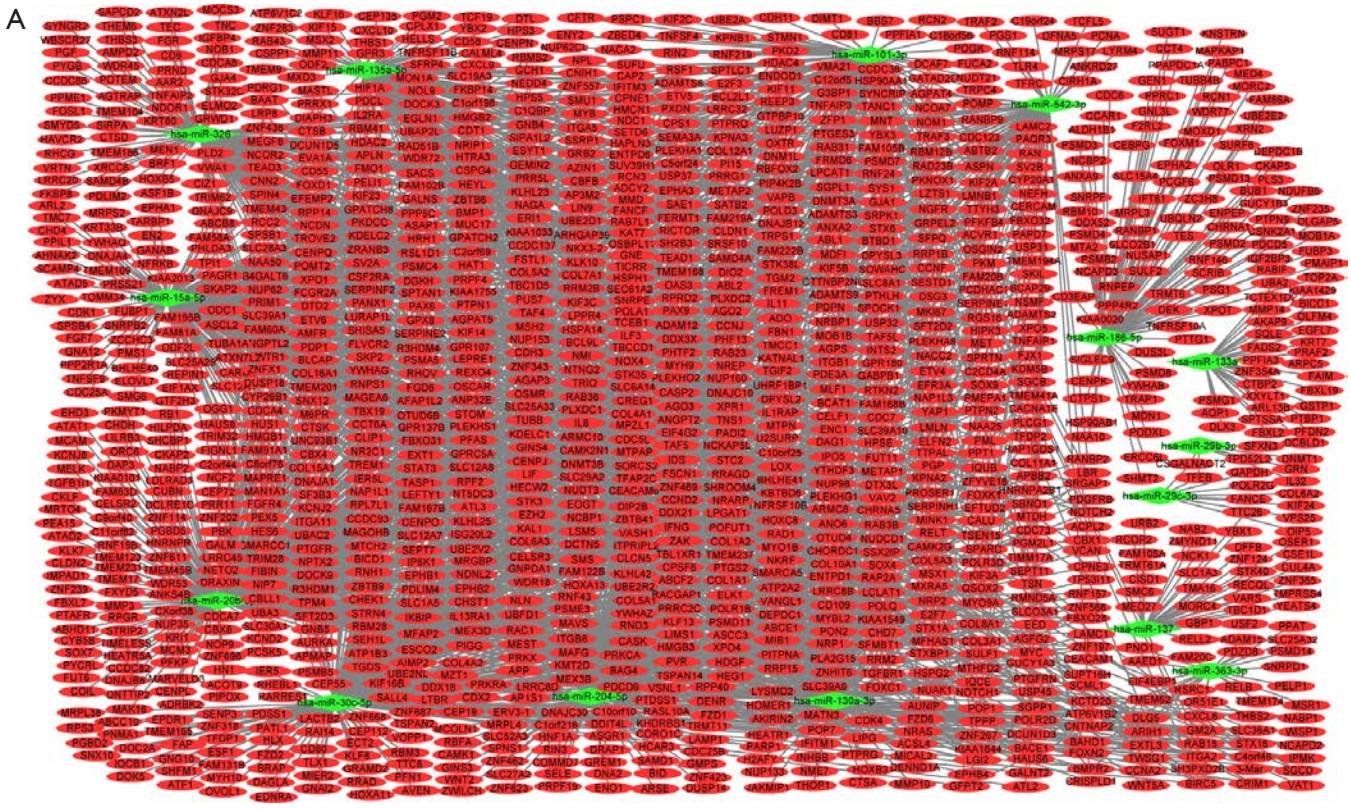

Figure 1 DEmiRNA-mRNA interaction network. (A) Six hundred and sixty-seven validated downregulated DEmiRNAs-upregulated DEmRNAs pairs; (B) 302 upregulated DEmiRNAs-downregulated DEmRNAs pairs. The rhombus represents DEmiRNAs, and the ellipse represents the target DEGs. Red colour represent upregulated DEmiRNAs or DEmRNAs, green colour represent downregulated DEmiRNAs or DEmRNAs. The lines indicate miRNAs-targets pairs with correlations. DEmiRNA, differentially expressed miRNA; DEmRNA, differentially expressed mRNA.

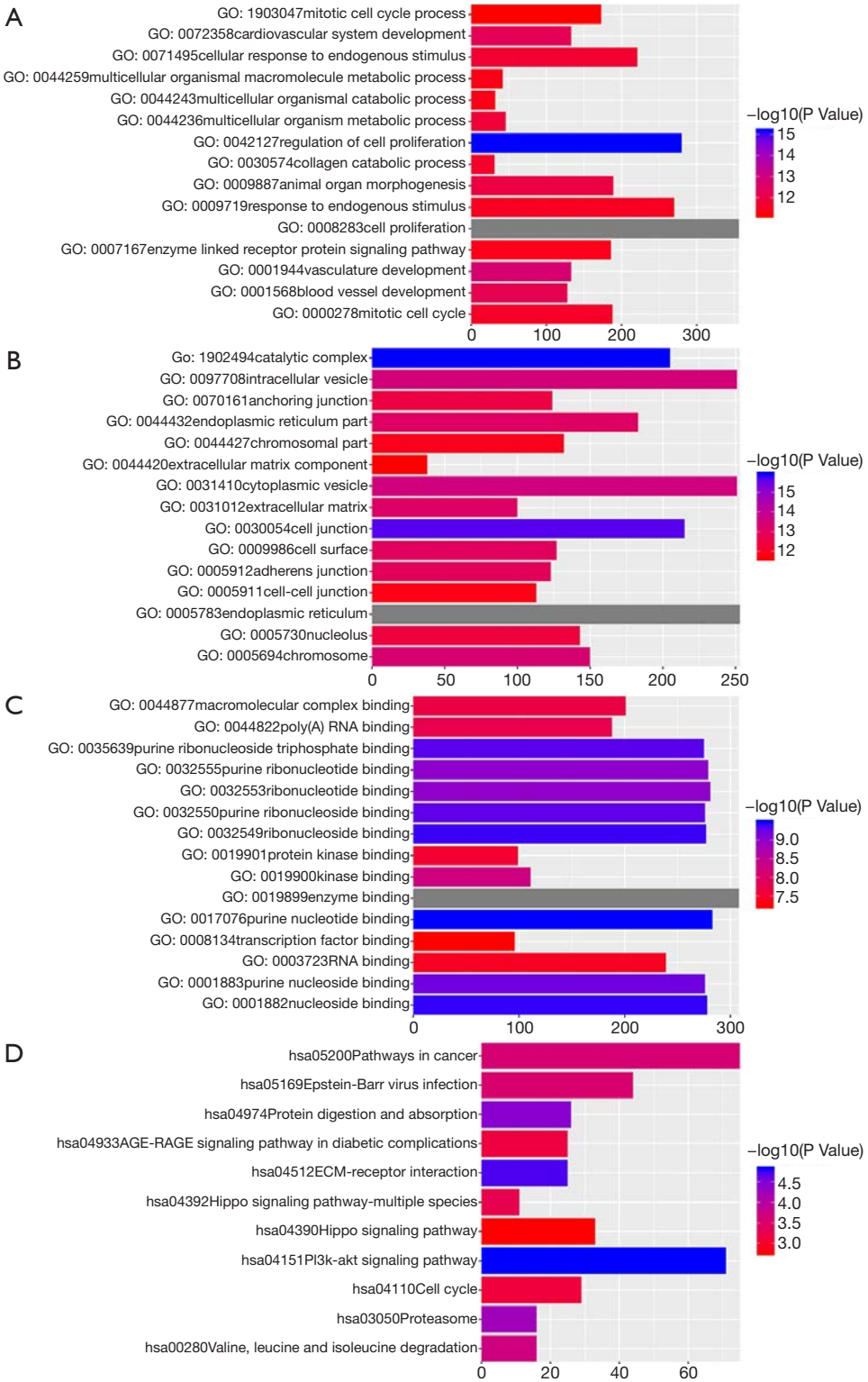

Figure 2 The top 15 most significantly enriched GO terms and KEGG pathways of target DEGs in gastric adenocarcinoma. The x-axis shows –log P and y-axis shows the terms of GO and KEGG. (A) Biological process. (B) cellular component; (C) molecular function; (D) KEGG.

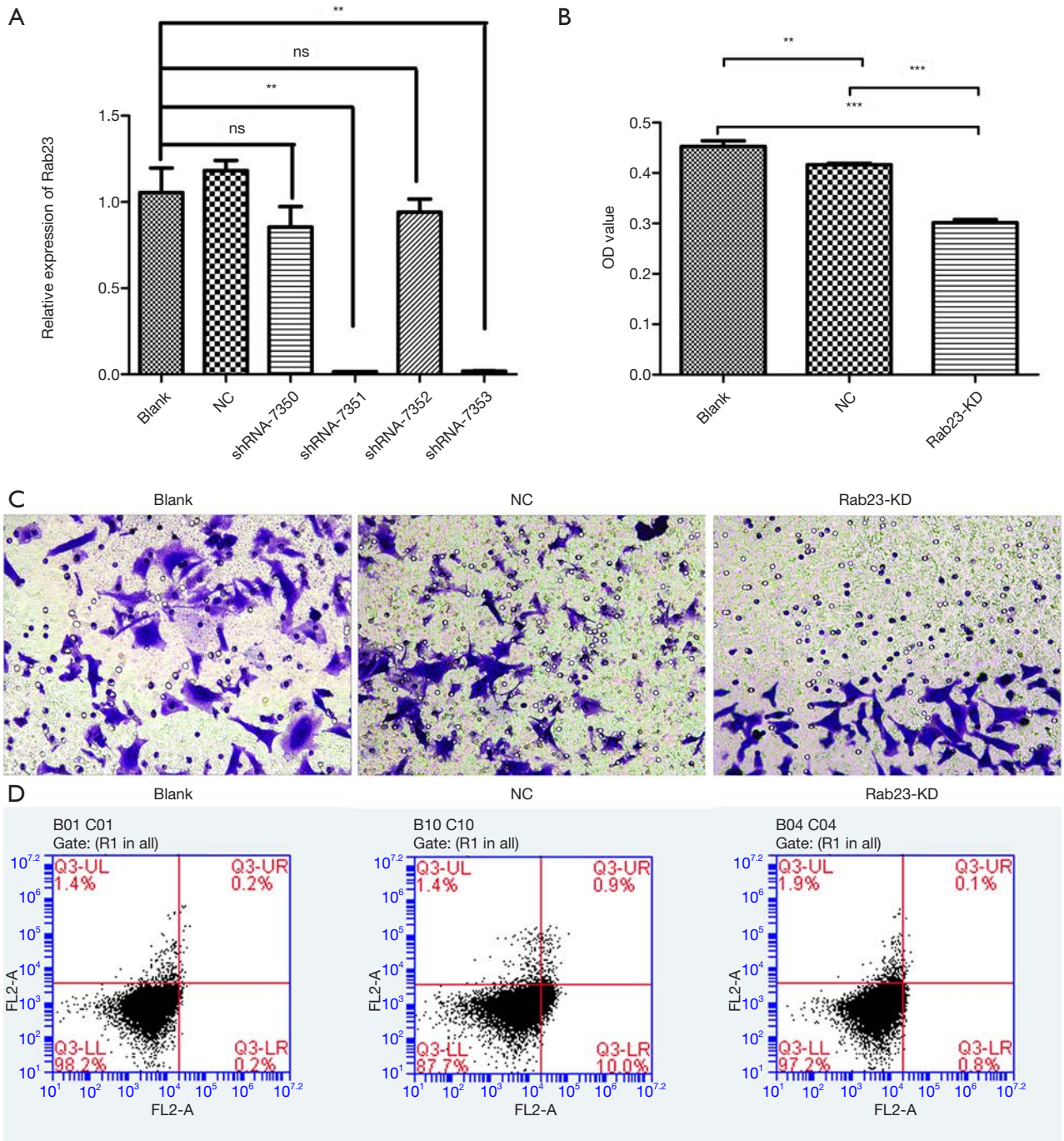

Figure 3 *RAB23* knockdown inhibits cell migration and invasion, promotes apoptosis of gastric cancer cells. (A) Expression of *RAB23* in MKN45 cell with or without shRNA. (B) cell proliferation of MKN45 cell with or without shRNA-7353 from CCK8 assay; (C) cell migration of MKN45 cell with or without shRNA-7353 was assessed using Transwell assay. (0.1% crystal violet staining, 400× magnification); (D) cell apoptosis of MKN45 cell with or without shRNA-7353 was evaluated using flow cytometry assay. Blank: cells without any treatment; NC: negative control, cells transfected with siRNA negative control; Rab23-KD: cells transfected with shRNA-RAB23. shRNA-7350, shRNA-7351, shRNA-7352 and shRNA-7353: cells transfected with shRNA-7350, shRNA-7351, shRNA-7352 and shRNA-7353. Results are from three repeated experiments. **, P<0.01; ***, P<0.001.

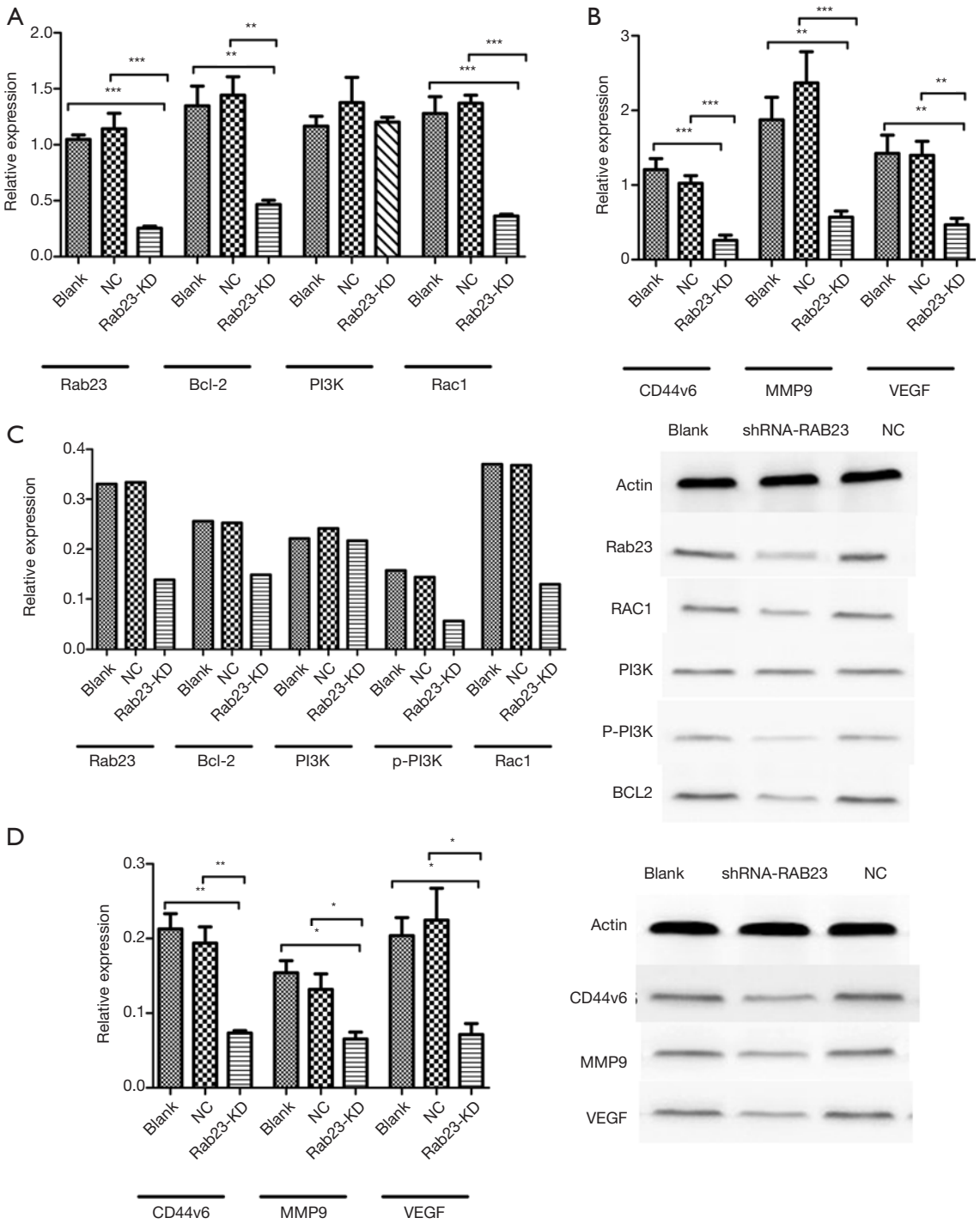

Figure 4 Expression of genes and proteins in MKN45 cell with or without shRNA-7353 by Western blot and RT-PCR. (A) the gene expression level of Rab23, Bcl-2, PI3K and Rac1 detected by RT-PCR; (B) the gene expression level of CD44v6, MMP9 and VEGF detected by RT-PCR; (C) the protein expression level of Rab23, Bcl-2, PI3K, p-PI3K and Rac1 detected by Western blot; (D) the protein expression level of CD44v6, MMP9 and VEGF detected by Western blot. Results are from three repeated experiments. *, P<0.05; **, P<0.01; ***, P<0.001. KD, knockdown; NC, negative control; RT-PCR, reverse transcription polymerase chain reaction.

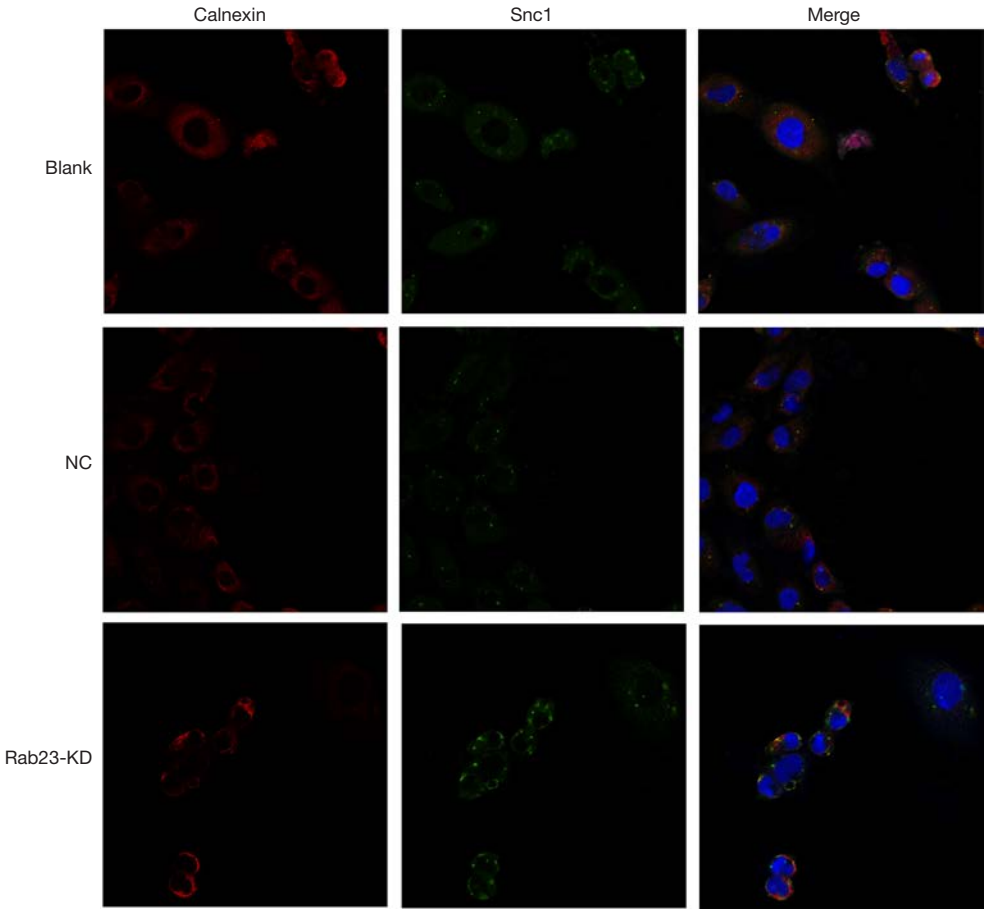

Figure 5 Colocalization analysis of Snc1 with vesicular protein VAMP3 and endoplasmic reticulum protein Calnoxin.

patients are diagnosed with disease at an advanced stage (23). As a consequence, the 5-year survival rate is extremely poor, at <10%, and this diagnosis at an advanced stage is partially due to a lack of identified early-stage diagnostic markers and efficient monitoring methods for cancer progression. In the present study, after integrated analysis, *RAB23* was indicated to be upregulated in gastric adenocarcinoma tissues compared to normal tissues, and this upregulation was affected by hsa-miR-130a-3p and hsa-miR-363-3p. We speculated that *RAB23* may be a potential noninvasive biomarker for the early diagnosis of gastric adenocarcinoma. To verify the function of *RAB23* in gastric adenocarcinoma cells, MKN45 cells were transfected with shRNA-*RAB23* to inhibit the expression of *RAB23*. Cell Counting Kit-8, transwell and flow cytometry assays were utilized to measure the cell proliferation, migration and apoptosis rate of cells, and gene and apoptosis-related protein expression levels were determined using PCR and Western blot assays.

In this study, we constructed a DEmRNAs-DEmiRNAs interaction network and identified several DEmRNA-DEmiRNA pairs involved in gastric adenocarcinoma. Based on the interaction network in this study, we identified three interactions, hsa-miR-23a-3p-*PTPN4*, hsa-miR-20b-5p (hsa-miR-130a-3p)-*TNFRSF10B*, and hsa-miR-130a-3p (hsa-miR-363-3p)-*RAB23*, that may be related to the pathogenesis of gastric adenocarcinoma.

PTPN4 is related to signal transduction, which regulates cell growth and differentiation, and regulates cell functions that promote apoptosis (24). The role of *PTPN4* in tumors has rarely been discussed, and one study showed that it negatively regulated cell proliferation and the movement of HeLa and Hep3B cells (25). Zhu *et al.* reported that miR-183 exerted a proinvasive effect by inhibiting the expression of *PTPN4*, which may be a new therapeutic target for inhibiting the metastasis of non-small-cell lung cancer tumor stem cells (26). In our present study, the decreased

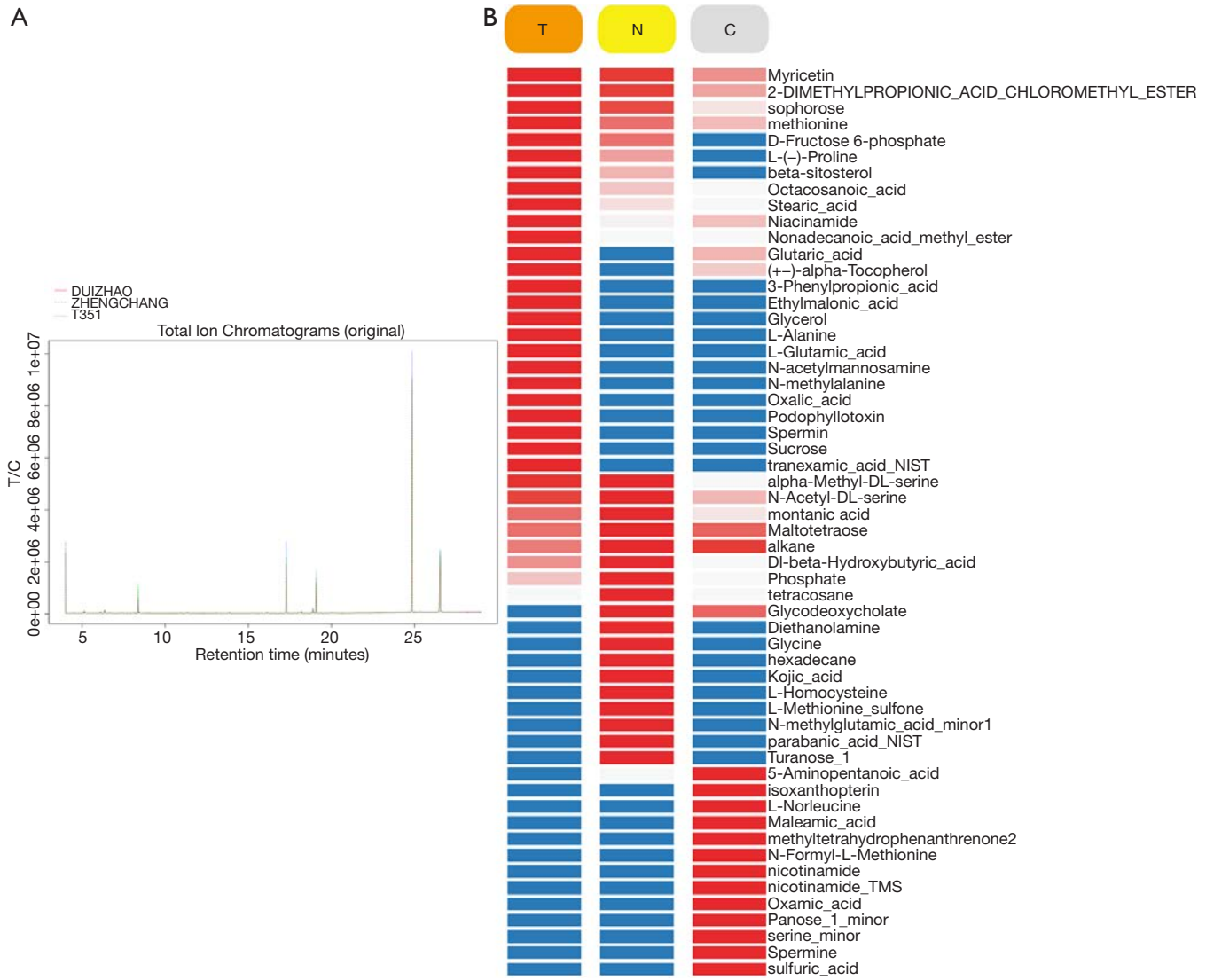

Figure 6 Metabolomic analysis was performed by using GC-MS. GC-MS, gas chromatography mass spectrometry.

expression of *PTPN4* in the tissues of patients with gastric adenocarcinoma compared to normal tissues was regulated by hsa-miR-23a-3p. This finding was in line with those of other studies and emphasized the significance of *PTPN4* in gastric adenocarcinoma. We speculated that *PTPN4* was involved in gastric adenocarcinoma and that its role was regulated by hsa-miR-23a-3p.

It is evident that *RAB23* overexpression plays a key role in malignant tumors (16). For instance, Jiang *et al.* (9) reported that overexpressed *RAB23* increased cell growth and invasion by increasing NF-kappa B signal transduction. Jian *et al.* (27) also reported that *RAB23* increased the migration and invasion of squamous cell carcinoma cells through the integrin 1/Rac1 pathway. More importantly, Hou *et al.* (22) found that *RAB23* promoted tumor progression in GC. In our integrated analysis, *RAB23* was significantly upregulated in tissues of patients with gastric adenocarcinoma compared to normal tissues, and this increased expression was regulated by hsa-miR-130a-3p and hsa-miR-363-3p based on the DEmiRNA-DEmRNA interaction network. Furthermore, in the GO and KEGG analyses, we found that *RAB23* was enriched in the GO terms "cytoplasmic vesicle" and "intracellular vesicle". *RAB23* was related to vesicle transport, as revealed by the immunofluorescence results. More relevant to our study, another recent report confirmed that *RAB23* was an

upregulated gene in nonmalignant gastric tissue compared to normal gastric mucosa (28). These findings confirm that upregulated *RAB23* may be related to an early stage of gastric carcinogenesis due to atrophic gastritis, which may increase the risk of GC. Importantly, Bin *et al.* (29) indicated that miR-367 overexpression inhibited the metastasis and invasion of gastric cancer by directly regulating *RAB23*. All of these data demonstrate the important role of *RAB23* in the pathogenesis of gastric adenocarcinoma.

Rac1 is a member of the Rac subfamily of the Rho family. Abnormal activation of GTPases has been shown to promote cancer cell movement, invasion and metastasis in several cancers (30). Jian *et al.* found that Rac1 activation was crucial for Rab23-induced hepatocellular carcinoma cell migration. Upregulated Rab23 efficiently increased the active Rac1 levels, while silencing Rab23 decreased Rac1 activation. When Rac1 was silenced, the increased Hep3B cell migration induced by Rab23 expression was significantly attenuated. In squamous cell carcinoma cells, Rab23 promoted migration and invasion by regulating the integrin β1/Tiam1/Rac1 pathway (27), and Rab23 promoted migration and invasion by regulating NF-κB in bladder cancer (9). In the present study, *RAB23* knockdown significantly reduced the expression level of Rac1. These findings demonstrated that Rab23 promoted gastric cancer cell migration via the PI3K-Akt signaling pathway by activating Rac1. We also speculate that Rab23 promotes the proliferation and metastasis of GC via multiple mechanisms and that Rab23 might be a useful molecular therapeutic target for gastric cancer. More studies should be performed to explore the regulation of Rab23 in gastric cancer.

Based on the GO and KEGG enrichment analyses, we found that the intracellular vesicle, vesicle-mediated transport and the PI3K-Akt signaling pathways were the most enriched pathways, and *RAB23* was enriched in the GO term intracellular vesicle. Abnormal PI3K/AKT signaling can cause cancer and other diseases. The PI3K-Akt signaling pathway regulates basic cellular functions such as transcription, translation, proliferation, growth and survival. Bcl-2 and Rac1 are involved in these processes (31). As originally reported by Wu *et al.* (32), the PI3K/AKT signaling pathway was found to be involved in cell migration *in vitro* and metastasis *in vivo* in gastric cancer. In the GO and KEGG analyses, the PI3K-Akt signaling pathway was the most significantly enriched pathway. Our *in vitro* study indicated that *RAB23* knockdown significantly reduced the expression of Bcl-2 and the tumor angiogenesis-promoting protein Rac1. There was no significant change in the level of PI3K protein or PI3K phosphorylation. Our immunofluorescence analysis also revealed that *RAB23* knockdown affected vesicle transport. *RAB23* was enriched in the GO term intracellular vesicle. The Rab protein is considered to be one of the crucial protein molecules involved in vesicle transport. Muniz *et al.* (33) found that in pancreatic cancer, the overexpression of RABL6A protein can promote the proliferation of tumor cells. Lin *et al.* (2) found that Rab25 regulated vesicle transport by changing the conformation of guanosine triphosphate, which plays an important role in the development of ovarian cancer. Jacob *et al.* (34) found that Rab40b was involved in the metastasis of breast cancer by regulating vesicle transport. Based on these findings, we speculated that hsa-miR-130a-3p and hsa-miR-363-3p regulate the expression of *RAB23* and affect the vesicle transport-related pathways in gastric cancer cells.

The results from the metabolic analysis revealed significantly altered metabolites, including glycerol, niacinamide, nonadecanoic acid methylester and methionine. Glycerol may serve a crucial purpose in cell growth and vitality by leading to the production of ATP and lipids (35,36). Studies have shown that damage to glycerin uptake leads to loss of T cell activity, which can be reversed by glycerin administration (35). We found that *RAB23* deficiency partially blocked glycerol uptake, and the decrease was associated with proliferation, injury and lipid synthesis. As mentioned earlier, there are significant differences in circulating levels of endogenous metabolites such as fatty acids, organic acids, carbohydrates, amino acids and steroids in patients with GC (37-39). These variations may indicate that the metabolism of tumor cells disrupts several metabolic pathways in patients.

In conclusion, we present evidence of the significance of *RAB23* as a diagnostic marker and a therapeutic target for human gastric adenocarcinoma. The PI3K/AKT pathway is involved in promoting cell growth, inhibiting apoptosis, promoting cell migration, and carrying out *RAB23*-mediated metabolic changes and is important for the etiology of the disease.

Acknowledgments

Funding: The study was funded by the National Key Clinical Specialist Construction Programs of China, Fujian Provincial Natural Science Foundation Projects (2019J01452) and Fujian Provincial Natural Science Foundation Projects (2017J01287).

Footnote

Conflicts of Interest: The authors have no conflicts of interest to declare.

Ethical Statement: The authors are accountable for all aspects of the work in ensuring that questions related to the accuracy or integrity of any part of the work are appropriately investigated and resolved.

References

1. Ferlay J, Soerjomataram I, Dikshit R, et al. Cancer incidence and mortality worldwide: sources, methods and major patterns in GLOBOCAN 2012. Int J Cancer 2015;136:E359-86.
2. Lin Y, Ueda J, Kikuchi S, et al. Comparative epidemiology of gastric cancer between Japan and China. World J Gastroenterol 2011;17:4421-8.
3. Park YH, Kim N. Review of atrophic gastritis and intestinal metaplasia as a premalignant lesion of gastric cancer. J Cancer Prev 2015;20:25-40.
4. Ng JY, Chan DK, Tan KK. Is gastroscopy for fecal immunochemical test positive patients worthwhile? Int J Colorectal Dis 2017;32:95-8.
5. Yan L, Wu K, Du F, et al. miR-384 suppressed renal cell carcinoma cell proliferation and migration through targeting RAB23. J Cell Biochem 2018. doi: 10.1002/jcb.27180.
6. Zhang L, Zhang B, You W, et al. Rab23 Promotes Hepatocellular Carcinoma Cell Migration Via Rac1/TGF-β Signaling. Pathol Oncol Res 2018. doi: 10.1007/s12253-018-0463-z.
7. Jiao ZH, Wang JD, Wang XJ. MicroRNA-16 suppressed the invasion and migration of osteosarcoma by directly inhibiting RAB23. Eur Rev Med Pharmacol Sci 2018;22:2598-605.
8. Cheng L, Yang F, Zhou B, et al. RAB23, regulated by miR-92b, promotes the progression of esophageal squamous cell carcinoma. Gene 2016;595:31-8.
9. Jiang Y, Han Y, Sun C, et al. Rab23 is overexpressed in human bladder cancer and promotes cancer cell proliferation and invasion. Tumour Biol 2016;37:8131-8.
10. Wang Y, Wu N, Liu J, et al. FusionCancer: a database of cancer fusion genes derived from RNA-seq data. Diagn Pathol 2015;10:131.
11. Stark C, Breitkreutz BJ, Reguly T, et al. BioGRID: a general repository for interaction datasets. Nucleic Acids Res 2006;34:D535-9.
12. Smoot ME, Ono K, Ruscheinski J, et al. Cytoscape 2.8: new features for data integration and network visualization. Bioinformatics 2011;27:431-2.
13. Lei Y, Guo P, Li X, et al. Identification of Differentially Expressed miRNAs and mRNAs in Vestibular Schwannoma by Integrated Analysis. Biomed Res Int 2019;2019:7267816.
14. Liu J, Liu F, Shi Y, et al. Identification of key miRNAs and genes associated with stomach adenocarcinoma from The Cancer Genome Atlas database. FEBS Open Bio 2018;8:279-94.
15. Chen C, Maimaiti A, Zhang X, et al. Knockdown of RAI14 suppresses the progression of gastric cancer. Onco Targets Ther 2018;11:6693-703.
16. Zhang XY, Mu JH, Liu LY, et al. Upregulation of miR-802 suppresses gastric cancer oncogenicity via targeting RAB23 expression. Eur Rev Med Pharmacol Sci 2017;21:4071-8.
17. Rollins J, Miskolci V. Immunofluorescence and subsequent confocal microscopy of intracellular TNF in human neutrophils. Methods Mol Biol 2014;1172:263-70.
18. Zhang HH, Gu GL, Zhang XY, et al. Primary analysis and screening of microRNAs in gastric cancer side population cells. World J Gastroenterol 2015;21:3519-26.
19. Song B, Yan J, Liu C, et al. Tumor Suppressor Role of miR-363-3p in Gastric Cancer. Med Sci Monit 2015;21:4074-80.
20. Tsai CL, Chiu YM, Ho TY, et al. Gallic Acid Induces Apoptosis in Human Gastric Adenocarcinoma Cells. Anticancer Res 2018;38:2057-67.
21. Tan X, Tang H, Bi J, et al. MicroRNA-222-3p associated with Helicobacter pylori targets HIPK2 to promote cell proliferation, invasion, and inhibits apoptosis in gastric cancer. J Cell Biochem 2018;119:5153-62.
22. Hou Q, Wu YH, Grabsch H, et al. Integrative genomics identifies RAB23 as an invasion mediator gene in diffuse-type gastric cancer. Cancer Res 2008;68:4623-30.
23. Badgwell B, Das P, Ajani J. Treatment of localized gastric and gastroesophageal adenocarcinoma: the role of accurate staging and preoperative therapy. J Hematol Oncol 2017;10:149.
24. Huai W, Song H, Wang L, et al. Phosphatase PTPN4 preferentially inhibits TRIF-dependent TLR4 pathway by dephosphorylating TRAM. J Immunol 2015;194:4458-65.
25. Zhou J, Wan B, Shan J, et al. PTPN4 negatively regulates CrkI in human cell lines. Cell Mol Biol Lett 2013;18:297-314.

26. Zhu C, Deng X, Wu J, et al. MicroRNA-183 promotes migration and invasion of CD133(+)/CD326(+) lung adenocarcinoma initiating cells via PTPN4 inhibition. Tumour Biol 2016;37:11289-97.
27. Jian Q, Miao Y, Tang L, et al. Rab23 promotes squamous cell carcinoma cell migration and invasion via integrin beta1/Rac1 pathway. Oncotarget 2016;7:5342-52.
28. Evans TM, Ferguson C, Wainwright BJ, et al. Rab23, a negative regulator of hedgehog signaling, localizes to the plasma membrane and the endocytic pathway. Traffic 2003;4:869-84.
29. Bin Z, Dedong H, Xiangjie F, et al. The microRNA-367 inhibits the invasion and metastasis of gastric cancer by directly repressing Rab23. Genet Test Mol Biomarkers 2015;19:69-74.
30. Bid HK, Roberts RD, Manchanda PK, et al. RAC1: an emerging therapeutic option for targeting cancer angiogenesis and metastasis. Mol Cancer Ther 2013;12:1925-34.
31. Pan Y, Wang N, Xia P, et al. Inhibition of Rac1 ameliorates neuronal oxidative stress damage via reducing Bcl-2/Rac1 complex formation in mitochondria through PI3K/Akt/mTOR pathway. Exp Neurol 2018;300:149-66.
32. Wu X, Chen Y, Li G, et al. Her3 is associated with poor survival of gastric adenocarcinoma: Her3 promotes proliferation, survival and migration of human gastric cancer mediated by PI3K/AKT signaling pathway. Med Oncol 2014;31:903.
33. Muniz VP, Askeland RW, Zhang X, et al. RABL6A Promotes Oxaliplatin Resistance in Tumor Cells and Is a New Marker of Survival for Resected Pancreatic Ductal Adenocarcinoma Patients. Genes Cancer 2013;4:273-84.
34. Jacob A, Jing J, Lee J, et al. Rab40b regulates trafficking of MMP2 and MMP9 during invadopodia formation and invasion of breast cancer cells. J Cell Sci 2013;126:4647-58.
35. Cui G, Staron MM, Gray SM, et al. IL-7-Induced Glycerol Transport and TAG Synthesis Promotes Memory CD8+ T Cell Longevity. Cell 2015;161:750-61.
36. Hara-Chikuma M, Verkman AS. Prevention of skin tumorigenesis and impairment of epidermal cell proliferation by targeted aquaporin-3 gene disruption. Mol Cell Biol 2008;28:326-32.
37. Ikeda A, Nishiumi S, Shinohara M, et al. Serum metabolomics as a novel diagnostic approach for gastrointestinal cancer. Biomed Chromatogr 2012;26:548-58.
38. Song H, Peng JS, Dong-Sheng Y, et al. Serum metabolic profiling of human gastric cancer based on gas chromatography/mass spectrometry. Braz J Med Biol Res 2012;45:78-85.
39. Yang T, Luo P, Li Y, et al. A serum metabolomics study of gastric cancer based on pseudotargeted liquid chromatography-mass spectrometry approach. Se Pu 2014;32:126-32.

Cite this article as: Chen H, Pan D, Yang Z, Li L. Integrated analysis and knockdown of *RAB23* indicate the role of *RAB23* in gastric adenocarcinoma. Ann Transl Med 2019;7(23):745. doi: 10.21037/atm.2019.11.130

Supplementary

Table S1 Top 20 differentially expressed mRNAs between gastric carcinoma tissues and adjacent normal tissues

ID	Symbol	Combined.ES	P value	FDR	UpDown
9076	CLDN1	2.518676164	0	0	Up
7070	THY1	2.395677941	0	0	Up
55959	SULF2	2.383579003	0	0	Up
1366	CLDN7	2.327402034	0	0	Up
7076	TIMP1	2.232796835	0	0	Up
51330	TNFRSF12A	2.191340955	2.22E-16	3.86E-14	Up
91461	PKDCC	2.1597033	8.88E-16	1.41E-13	Up
4913	NTHL1	2.122437085	1.33E-15	2.00E-13	Up
27043	PELP1	2.082010138	6.66E-15	8.78E-13	Up
26528	DAZAP1	2.074501176	7.11E-15	9.16E-13	Up
495	ATP4A	–5.006828519	0	0	Down
2104	ESRRG	–4.226611973	0	0	Down
135892	TRIM50	–4.066034428	0	0	Down
887	CCKBR	–4.023543347	0	0	Down
2694	GIF	–3.992196723	0	0	Down
9992	KCNE2	–3.842617254	0	0	Down
1358	CPA2	–3.819030328	0	0	Down
440556	LINC00982	–3.616788411	0	0	Down
4118	MAL	–3.472888379	0	0	Down
222235	FBXL13	–3.462400246	0	0	Down

FDR, false discovery rate.

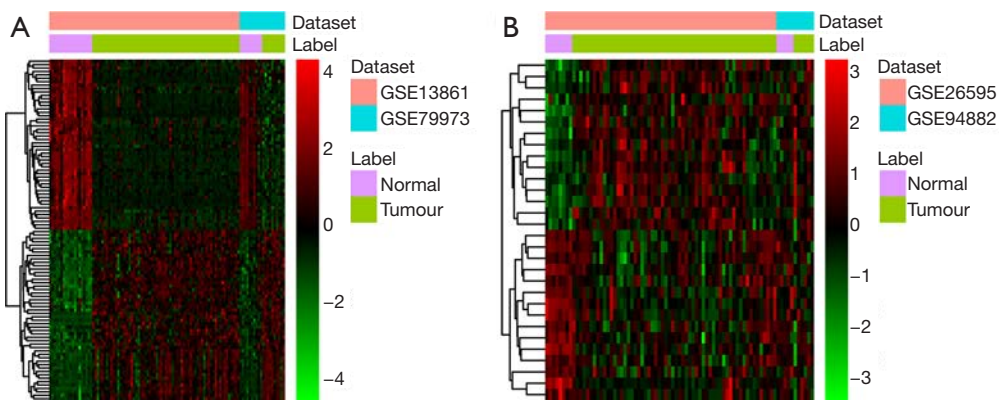

Figure S1 Heat-map image displaying the top 100 DEGs and DEmiRNAs that were significantly up-regulated or down-regulated (P<0.05) in gastric adenocarcinoma tissues compared to normal tissues. (A) DEGs; (B) DEmiRNAs. DEGs, differentially expressed genes; DEmiRNA, differentially expressed miRNA.

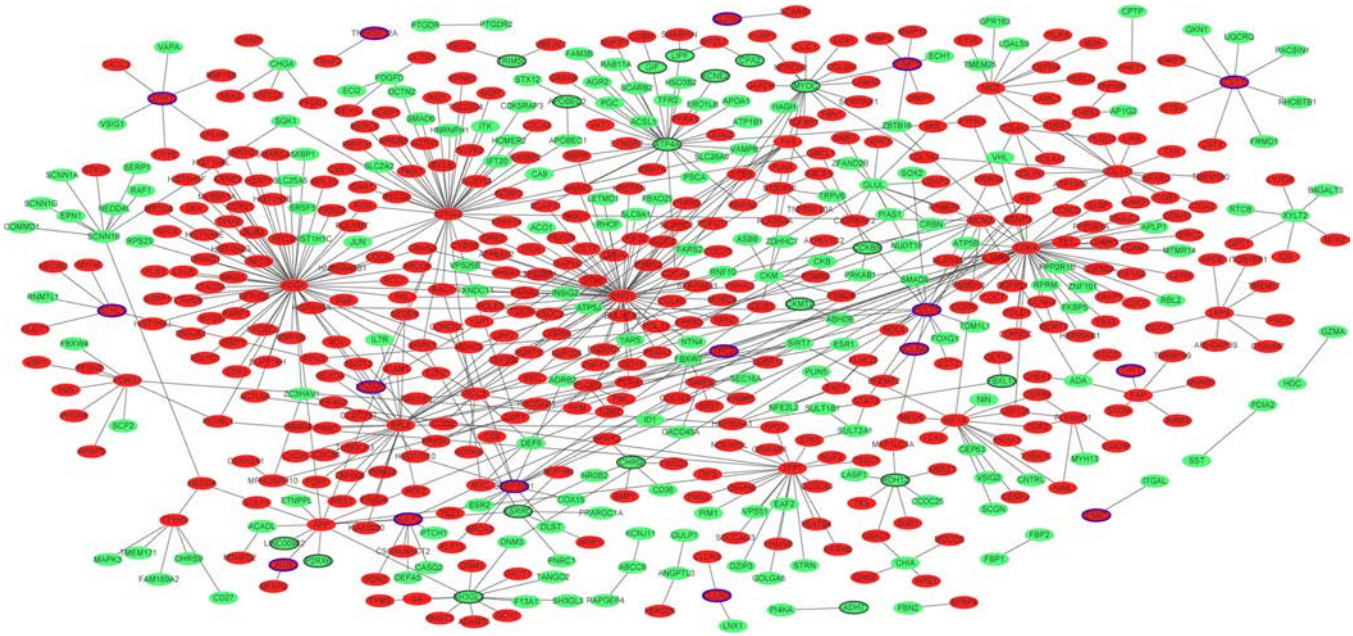

Figure S2 GC-specific protein-protein interaction network. Red and green ellipses represent proteins encoded by up- and down-regulated DEGs, respectively. Edges indicate integrations between proteins. Blue ellipses represent other proteins. DEGs, differentially expressed genes; GC, gas chromatography.

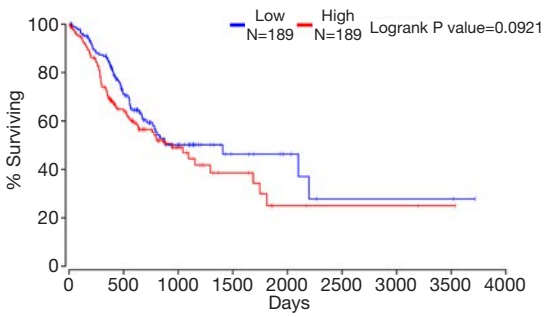

Figure S3 Overall survival analysis in GAC based on the TCGA data as determined by. Survival curves of RAB23 by univariate Cox regression analysis. Kaplan-Meier estimates (log-rank test) were made and found the expression of RAB23.

Table S2 Top 20 differentially expressed miRNAs between gastric carcinoma tissues and adjacent normal tissues

Symbol	Combined.ES	P value	FDR	UpDown
hsa-miR-135b-5p	2.411406499	5.33E-10	3.67E-08	Up
hsa-miR-425-5p	1.954423418	1.74E-07	4.80E-06	Up
hsa-miR-181c-5p	1.901387702	3.32E-07	7.55E-06	Up
hsa-miR-23a-3p	1.576200036	7.96E-06	0.000109866	Up
hsa-miR-197-3p	1.438758908	4.14E-05	0.000412366	Up
hsa-miR-181b-5p	1.484959414	4.18E-05	0.000412366	Up
hsa-miR-224-5p	1.433213685	4.54E-05	0.000417767	Up
hsa-miR-10a-5p	1.491875273	5.99E-05	0.000470771	Up
hsa-miR-18a-3p	1.368261508	0.000168255	0.001105673	Up
hsa-miR-214-3p	1.161427594	0.00122815	0.006053026	Up
hsa-miR-204-5p	–3.086768205	5.41E-13	7.47E-11	Down
hsa-miR-363-3p	–2.190803804	1.43E-08	6.58E-07	Down
hsa-miR-30c-5p	–2.080027306	7.95E-08	2.74E-06	Down
hsa-miR-20b-5p	–1.867359692	7.05E-07	1.08E-05	Down
hsa-miR-29c-3p	–1.524917472	2.05E-05	0.000257408	Down
hsa-miR-29b-3p	–1.442591448	6.38E-05	0.000470771	Down
hsa-miR-186-5p	–1.398074249	6.82E-05	0.000470771	Down
hsa-miR-133a	–1.281172099	0.000325219	0.001951315	Down
hsa-miR-130a-3p	–1.082787295	0.001224211	0.006053026	Down
hsa-miR-137	–1.126028682	0.001388646	0.006608037	Down

FDR, false discovery rate.